Physics and Device Performance of Superconducting Nanowire Single-Photon Detectors

Taro YAMASHITA

Recently, in the various fields such as quantum communication, superconducting nanowire single-photon detectors (SSPD) attract much attention because of their many merits, e.g., high counting rate and so on. However, several parts of important fundamental physics in SSPDs has not been clarified yet. In this work, we measured and analyzed the dark count (error count) of the SSPD in a wide temperature range, and identified its physical origin.

1 Introduction

In recent years there has been a rapid rise in demand for high performance single photon detectors in a wide variety of research fields including quantum communication and quantum optics[1][2]. Research has so far been carried out on single photon detectors, including numerous types of devices using photomultipliers and semiconductors. Superconducting nanowire single-photon detectors (SSPD) attract a lot of attention as the current mainstream in this research[3][4]. The SSPD has numerous outstanding characteristics, including rapid response, broadband performance, high detection efficiency, and low timing jitter, outperforming other single photon detectors such as the avalanche photodiode. Experimental results of unprecedented precision are already being achieved in a variety of research fields as the result of using the SSPD. For example, field tests of quantum key distribution have succeeded in dramatically improving transmission distances and key generation rates through its use[2]. So far we had built high-performance and practical SSPD systems for application in a variety of fields, including tests of key distribution using quantum cryptography.

The performance of the SSPD has improved rapidly over the past few years, but on the other hand, there are many parts of the physical mechanism behind the SSPD which remain unexplained. One of the most significant is the physical origin of "dark counts", which is a vital performance factor of the SSPD. The dark count is the error count without incident light. Needless to say the ideal is for it to be zero. As shown in Fig. 1, the output signal of the SSPD is produced as the result of local resistance generated by the transition of a part of the superconducting nanowire of zero resistance to a state of normal conduction. For this reason, it is important to clarify the physical mechanism behind the spontaneous generation of resistance (despite the absence of incident light) in order to elucidate the origin of the dark count. The sensitivity and detection efficiency of the SSPD increases with a rise in the bias current. But the dark count is also known to increase with a rise in the bias current. For this reason, the vital point in drawing out the full potential of the SSPD is how the dark count can be suppressed. So far the physical mechanism behind how the dark count is being generated had remained unexplained, and no specific methods for suppressing it existed. We measured the dark count at a wide-range of temperatures with the aim of elucidating its origin, then analyzed the results of those experiments using theoretical models[5].

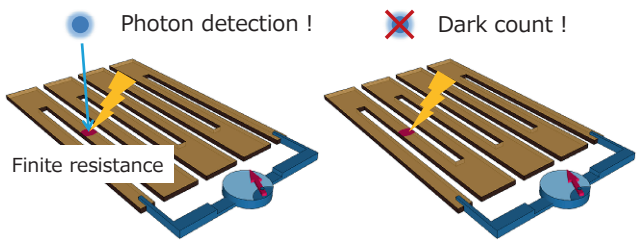

Fig. 1 Photon detection and dark count in the SSPD

2 Two-dimensional superconductors and vortex motion

One of the candidates for the mechanism behind how the dark count is generated is the transition to a state of resistance created by a vortex (decoherence). The SSPD is an ultrathin film 4 to 5 nm thick, and the coherence length

of the niobium nitride (NbN) thin film used in the SSPD is around 5 nm, making it about the same thickness as the SSPD film. This allows the SSPD to be treated as a two-dimensional superconductor. There is no resistance in two-dimensional superconductors if they are in a state of superconductivity, but if for some reason a vortex is created in the superconducting thin film, it moves through the thin film (vortex flow) generating temporary, local resistance. One of the first reasons that we can think of as to how vortices get into thin films is the intrusion of external magnetic fields. However, this possibility can be eliminated because the dark count is known to exist even when magnetic shields made of μ-metal for example, are used to protect the SSPD from the effects of external magnetic fields. A possibility as to why vortices are created even in the absence of an external magnetic field is the existence of fluctuations in vortices characteristic of two-dimensional superconductors. As shown in Fig. 2, there are mainly two mechanisms for these fluctuations. One is vortex hopping from an edge of the nanowire due to its own magnetic field generated around a bias current (Fig. 2(a)). A potential known as an edge barrier exists due to the requirements of boundary conditions relative to the magnetic field in nanowires, which works to eliminate vortices from nanowires. On the other hand, a Lorentz force by the bias current acts on the vortex to enter the nanowire. Thus, there is a competition between these two forces, and the probability of the vortex hopping increases as the bias current is increased. The other mechanism is the possibility of spontaneous generation of vortex-antivortex pairs within the thin film due to a phase transition known as the Berezinskii-Kosterlitz-Thouless (BKT) transition[6][7]. A dark count can occur in a process whereby a vortex flow is generated as vortex-antivortex pairs, resulting from a BKT transition, become unbound by the Lorentz force from the bias current (Fig. 2(b)). From these perspectives, we shall consider the origin of the dark count by examining (i) vortex hopping generated by the magnetic field of the bias current, and (ii) the two mechanisms behind the unbinding of vortex-antivortex pairs.

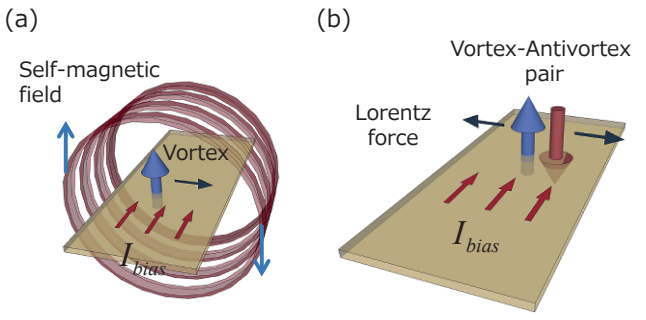

Fig. 2 (a) Vortex created by bias current's own magnetic field (b) Vortex-antivortex pair created by a BKT transition

3 Experimental setup

The SSPD device was fabricated by forming an NbN film on a single-crystal magnesium oxide (MgO) substrate by reactive DC magnetron sputtering in a meander pattern. The film was 4 nm in thickness, and the surface area of the meandering section was 20 μm × 20 μm, with a line width of w = 100 nm and spaces between nanowires of 60 nm. The critical current density, J_C, was 3.1×10^{10}A/m^2 at 3.0 K, with penetration depth λ (0) = 495 nm, and Ginzburg-Landau (GL) coherence length ξ (0) = 5 nm at absolute zero[8]. How the SSPD was made has been described in detail in another document[9].

A dilution refrigerator at a base temperature of 11 mK was used to measure the dark count. The sample stage equipped with an SSPD was vibration-free, and magnetically shielded by a double μ-metal shield. The device was current-biased via the DC arm of the bias tee, and the output signal passing through the AC arm of the bias tee and two low-noise amplifiers was observed using the pulse counter. With regard to the operating temperature, control through a Proportional-Integral-Derivative (PID) allows stable operations at the set temperature with deviations of less than ± a few mK to several tens of mK. In addition, measurements were carried out regarding DC characteristics in a cryofree He3 refrigerator. As with the dilution refrigerator, the sample stage was magnetically shielded with μ-metal, and the temperature could be controlled through a PID controller.

4 Experimental results and analysis I: BKT transition

Before starting discussions on the dark count, there is a need to confirm whether BKT transitions are actually taking place in the SSPD device. To confirm the presence of BKT transitions, the temperature dependence of current-voltage (IV) characteristics and resistance are normally measured[10]. Figure 3 shows the IV characteristics from 8.4 K to 9.0 K as measured by the standard four-terminal method. The temperature dependence of index α (T) is calculated by curve fitting these IV characteristics using the power-law formula (Fig. 3 inset). As it can be seen in the

figure, there is a sudden rise in the value at 8.50 K corresponding to $\alpha = 3$. This suggests the occurrence of BKT transition at this temperature (T_{BKT} = 8.50 K). T_C = 9.0 K can also be calculated from the fact that IV characteristics become linear (α = 1) at the superconducting transition temperature T_C. The index α (T) jumps from 3 to 1 in an ideal BKT transition, but a broad temperature dependence, as shown in the Fig. 3 inset, has been reported in systems with limited line width.

Beasley, Mooij, and Orlando presented the equation[11]

$$\frac{T_{BKT}}{T_C} = \left(1 + 0.173\varepsilon_{BKT}\frac{e^2 R_{SN}}{\hbar}\right)^{-1}, \quad (1)$$

to express the relation between the BKT transition temperature and superconducting transition temperature. Here, R_{SN} is sheet resistance under normal conduction conditions, and ε_{BKT} is the polarization constant of the vortex at the BKT transition temperature. When T_{BKT}, R_{SN} and T_C measurements are inserted (Fig. 3) into this Equation (1), ε_{BKT} = 2.15 is obtained.

The temperature dependence of sheet resistance R_s is shown in Fig. 4. The following equation is known to hold true in temperature ranges whereby $T_{BKT} < T < T_C$ [10].

$$R_S(T) = a\exp\left(-2\sqrt{b\frac{T_C - T}{T - T_{BKT}}}\right), \quad (2)$$

In the equation, a and b are fitting parameters. T_C = 9.0 K obtained from the IV characteristics is inserted into Equation (2), and the measurements from experiments in Fig. 4 are fitted to obtain T_{BKT} = 8.53 K, which turned out to be consistent with 8.50 K obtained from the IV characteristics. From these results, it was confirmed that BKT transitions were actually occurring in the SSPD device examined, and that vortex-antivortex pairs were being formed spontaneously in the nanowires.

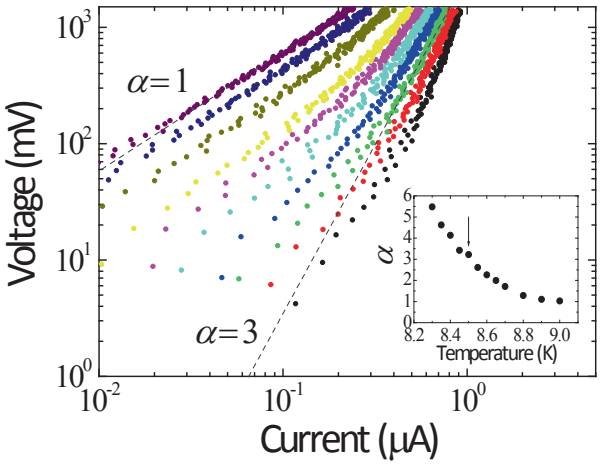

Fig. 3 Current-voltage characteristics. Showing characteristics, from right to left at 8.40, 8.45, 8.50, 8.55, 8.60, 8.65, 8.70, 8.80, 8.90, 9.00 K. Inset: The temperature dependence of α obtained from curve fitting based on the equation $V \propto I^{\alpha}$

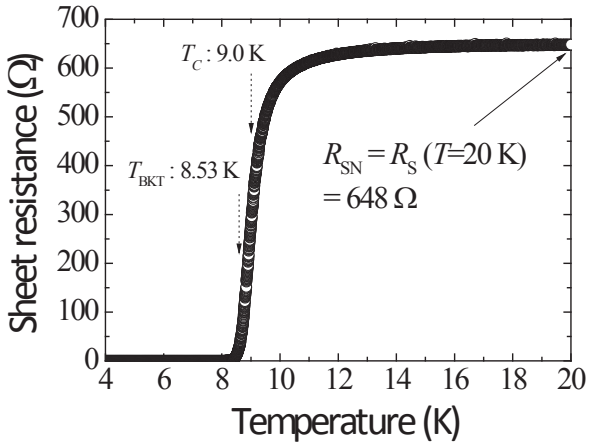

Fig. 4 Temperature dependence of sheet resistance

5 Experimental results and analysis II: Dark count

Next, we will discuss the origin of the dark counts. Figure 5 (symbols within the figure) shows the measured dependence of the dark count rate against a normalized bias current. Measurements were taken in the temperature range of 0.5 K to 4.0 K, and the bias current was normalized at each temperature by a superconducting critical current. It can be seen in Fig. 4 that the dark count

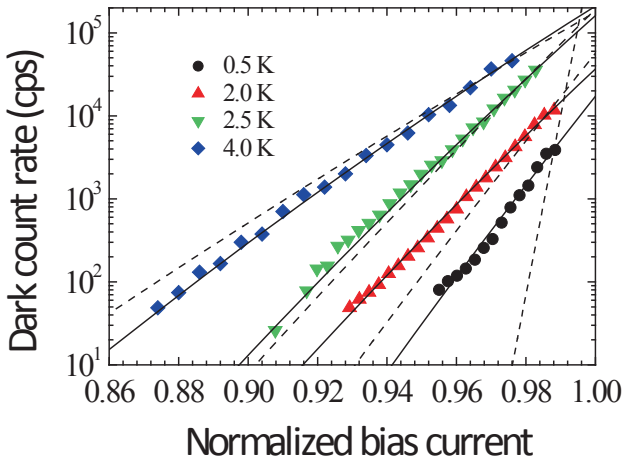

Fig. 5 Normalized bias current dependence of the dark count rate. Symbols indicate experimental measurements. The dashed lines show the best-fitting curves obtained from the vortex hopping model caused by its own magnetic field. The solid lines show the best-fitting curves obtained from the vortex-antivortex unbinding model.

increases uniformly in relation to the bias current at all temperatures, and the dark count decreases as the temperature decreases.

5.1 Vortex hopping due to self magnetic field

First we will examine vortex hopping caused by the magnetic field of the bias current itself. The edge barrier of the vortex generated on the edge of the nanowire can be expressed as a function x, indicating its position in the nanowire as shown below[12][13]:

$$U_{\mathrm{VH}}(x) = E_B\left[\ln\left(\frac{2w}{\pi\xi}\sin\left(\frac{\pi x}{w}\right)\right) + \frac{I_b}{I_B}\frac{\pi}{w}\left(x - \frac{\xi}{2}\right)\right], \quad (3)$$

Here, Equation (1) and Equation (2) are the temperature dependent GL coherence lengths[14]. The maximum value of the edge barrier $U_{\mathrm{VH,max}}$ can be derived from the conditional expression $\mathrm{d}U_{\mathrm{VH}}/\mathrm{d}x = 0$ as shown below:

$$U_{\mathrm{VH,max}} = E_B \ln\left\{\left[\frac{2w}{\pi\xi(T)}\left(1+\left(\frac{I_b}{I_B(T)}\right)^2\right)^{-1/2}\right] - \frac{I_b}{I_B}\left[\arctan\left(\frac{I_B}{I_b}\right) - \frac{\pi\xi}{2w}\right]\right\}, \quad (4)$$

Using Equation (4), the dark count rate resulting from vortex hopping can be expressed as:

$$P_{\mathrm{VH}}(T, I_b) = \Gamma_{\mathrm{att,VH}} I_{b\mathrm{N}} \exp\left(-\frac{U_{\mathrm{VH,max}}}{k_B T}\right), \quad (5)$$

Here $\Gamma_{\mathrm{att,VH}}$ is the attempt rate, and $I_{b\mathrm{N}}$ is the normalized bias current. The dashed lines in Fig. 5 show the fitting curves obtained from Equation (5) of the measurements taken during the experiment. As the figure clearly shows, it was ascertained that the vortex hopping model could not account for the dependence of the dark count rate on the bias current across all temperature ranges.

5.2 Unbinding of vortex-antivortex pairs

Next we will examine the possibility of the unbinding of vortex-antivortex pairs that are generated in nanowires as the result of BKT transitions. The potential of vortex-antivortex pairs while an electrical current is being applied can be expressed as below[10]:

$$U_{\mathrm{VAP}} = 2\mu_C + \frac{A(T)}{\varepsilon}\left[\ln\left(\frac{2.6I_C}{I_b}\right) - 1 + \frac{I_b}{2.6I_C}\right], \quad (6)$$

Here I_b is the bias current, I_C is the superconducting critical current, μ_C is the core potential of the vortex, and ε is the dielectric constant. Furthermore, $A(T) = \Phi_{02}/\pi\mu_0\Lambda(T)$, Φ_0 is a flux quantum, μ_0 is the magnetic permeability of vacuum, and $A(T)$ is the effective penetration depth[14]. Using this potential (6), the dark count rate resulting from the unbinding of vortex-antivortex pairs generated by the bias current can be expressed as below:

$$P_{\mathrm{VAP}}(T, I_b) = \Gamma_{\mathrm{att,VAP}} \exp\left(-\frac{U_{\mathrm{VAP}}}{k_B T}\right), \quad (7)$$

Here $\Gamma_{\mathrm{att,VAP}}$ is the attempt rate, and k_B is the Boltzmann constant. The solid lines in Fig. 5 show the hypothetical curves obtained from fitting Equation (7) to the experimental results by the least-squares method. As seen in the figure, it fits extremely well to the experimental results across all temperature ranges. In addition, the values of the fitting parameter ε obtained from this fitting were 1.5 to 6.5, which were comparable to the value of $\varepsilon_{\mathrm{BKT}}$ = 2.15 calculated from the DC characteristics using Equation (1). This demonstrated that the unbinding model of vortex-antivortex pairs due to the bias current gave a good explanation of the experimental results.

From these observations, it was clarified that the physical origin of the dark count in the SSPD was the unbinding of vortex-antivortex pairs due to the bias current[5]. As it can be seen in Fig. 5, the unbinding model of vortex-antivortex pairs and the vortex hopping model show relatively similar dependence on the bias current at 2.5 K, making it difficult to identify which mechanism is the dominant origin of the dark count from measurements taken at this temperature. For this reason, the kind of measurement and analysis of temperature dependence we carried out is important in identifying the origin of the dark count.

6 Conclusion

In this work, we investigated the bias current dependence of the DC characteristics and the dark count of the SSPD at temperatures ranging from 0.5 K to 4.0 K. The obtained results were then analyzed using two theoretical models: (i) vortex hopping due to the bias current's self-magnetic field, and (ii) the unbinding of vortex-antivortex pairs generated by BKT transitions. As a result, it was clarified that the physical origin of the dark count was the unbinding of vortex-antivortex pairs. In order to develop dark-count-free SSPDs in the future, it will be necessary to suppress the unbinding of vortex pairs, or to invent novel structures that restrict the movement of isolated, individual vortices through pinning for example. The development of a dark-count-free SSPD will promote the development of quantum communication systems and fundamental experiments of quantum optics.

References

1 R.H. Hadfield, M.J. Stevens, S.S. Gruber, A.J. Miller, R.E. Schwall, R.P. Mirin, and S.W. Nam, "Single photon source characterization with a superconducting single photon detector," Opt. Express, Vol. 13, No. 26, pp. 10846–10853, 2005.

2 M. Sasaki, M. Fujiwara, H. Ishizuka, W. Klaus, K. Wakui, M. Takeoka, S. Miki, T. Yamashita, Z. Wang, A. Tanaka, K. Yoshino, Y. Nambu, S. Takahashi. A. Tajima, A. Tomita, T. Domeki, T. Hasegawa, Y. Sasaki, H. Kobayashi, T. Asai, K. Shimizu, T. Tokura, T. Tsurumaru, M. Matsui, T. Honjo, K. Tamaki, H. Takesue, Y. Tokura, J.F. Dynes, A.R. Dixon, A.W. Sharpe, Z.L. Yuan, A.J. Shields, S. Uchikoga, M. Legire, S. Robyr. P. Trinkler, L. Monat, J.-B. Page, G. Ribordy, A. Poppe, A. Allacher, O. Maurhart, T. Langer, M. Peev, and A. Zeilinger, "Field test of quantum key distribution in the Tokyo QKD Network," Optics Express Vol. 19, No. 11, pp. 10387–10409, 2011.

3 G.N. Gol'tsman, O. Okunev, G. Chulkova, A. Lipatov, A. Semenov, K. Smirnov, B. Voronov, A. Dzardanov, C. Williams, and Roman Sobolewski, "Picosecond superconducting single-photon optical detector," Appl. Phys. Lett. Vol. 79, No. 6, pp. 705–707, 2001.

4 R.H. Hadfield, "Single-photon detectors for optical quantum information applications," Nature Photonics, Vol. 3, No. 12, pp. 696–705, 2009.

5 T. Yamashita, S. Miki, K. Makise, W. Qiu, H. Terai, M. Fujiwara, M. Sasaki, and Z. Wang, "Origin of intrinsic dark count in superconducting nanowire single-photon detectors," Appl. Phys. Lett. Vol. 99, No. 16, pp. 161105, 2011.

6 Z.L. Berezinskii, "Destruction of long-range order in one-dimensional and two-dimensional systems having a continuous symmetry group I. Classical systems," Sov. Phys. JETP, Vol. 32, No. 3, pp. 493–500, 1971.

7 J.M. Kosterlitz and D.J. Thouless, "Ordering, metastability and phase transitions in two-dimensional systems," J. Phys. C, Vol. 6, pp. 1181–1203, 1973.

8 Z. Wang, A. Kawakami, Y. Uzawa, and B. Komiyama, "Superconducting properties and crystal structure of single-crystal NbN thin films deposited at ambient substrare temperature," J. Appl. Phys, Vol. 79, No. 10, pp. 7837–7842, 1996.

9 S. Miki, M. Fujiwara, M. Sasaki, and Z. Wang, "NbN Superconducting Single-Photon Detectors Prepared on Single-Crystal MgO Substrates," IEEE Trans. Appl. Supercond., Vol. 17, No. 2, pp. 285–288, 2007.

10 J.E. Mooij, "Two-dimensional transition in superconducting films and junction arrays, in Percolation, Localization, and Superconductivity," edited by A.M. Goldman and S.A. Wolf, pp. 325–370, Plenum, New York, 1984.

11 M.R. Beasley, J.E. Mooij, and T.P. Orlando, "Possibility of Vortex-Antivortex Pair Dissociation in Two-Dimensional Superconductors," Phys. Rev. Lett. Vol. 42, No. 17, pp. 1165–1168, 1979.

12 G.M. Maksimova, "Mixed state and critical current in narrow semiconducting films," Phys. Solid State, Vol. 40, No. 10, pp. 1607–1610, 1998.

13 H. Bartolf, A. Engel, A. Schilling, K. Il'in, M. Siegel, H.-W. Hubers, and A. Semenov, "Current-assisted thermally activated flux liberation in ultrathin nanopatterned NbN superconducting meander structures," Phys. Rev. B, Vol. 81, No. 2, pp. 024502, 2010.

14 M. Tinkham, "Introduction to Superconductivity," 2nd ed., McGraw-Hill, New York, 1996.

Taro YAMASHITA, Dr. Sci.

Senior Researcher, Nano ICT Laboratory,
Advanced ICT Research Institute
Superconducting Technology,
Theoretical Physics
taro@nict.go.jp